JOURNAL OF Applied Polymer SCIENCE

A Redox-Mediator-Doped Gel Polymer Electrolyte Applied in Quasi-Solid-State Supercapacitors

Fuda Yu, Miaoliang Huang, Jihuai Wu, Zhaoyuan Qiu, Leqing Fan, Jianming Lin, Yibing Lin
Engineering Research Center of Environment-Friendly Functional Materials, Ministry of Education, Institute of Materials Physical Chemistry, Huaqiao University, Quanzhou, 362021, Fujian, China
Correspondence to: M. Huang (E-mail: huangml@hqu.edu.cn)

ABSTRACT: Methylene blue (MB) redox mediator was introduced into polyvinyl alcohol/polyvinyl pyrrolidone (PVA/PVP) blend host to prepare a gel polymer electrolyte (PVA-PVP-H_2SO_4-MB) for a quasi-solid-state supercapacitor. The electrochemical properties of the supercapacitor with the prepared gel polymer electrolyte were evaluated by cyclic voltammetry, galvanostatic charge–discharge, electrochemical impedance spectroscopy, and self-discharge measurements. With the addition of MB mediator, the ionic conductivity of gel polymer electrolyte increased by 56% up to 36.3 $mS \cdot cm^{-1}$, and the series resistance reduced, because of the more efficient ionic conduction and higher charge transfer rate, respectively. The electrode specific capacitance of the supercapacitor with PVA-PVP-H_2SO_4-MB electrolyte is 328 $F \cdot g^{-1}$, increasing by 164% compared to that of MB-undoped system at the same current density of 1 $A \cdot g^{-1}$. Meanwhile, the energy density of the supercapacitor increases from 3.2 to 10.3 $Wh \cdot kg^{-1}$. The quasi-solid-state supercapacitor showed excellent cyclability over 2000 charge/discharge cycles. © 2013 Wiley Periodicals, Inc. J. Appl. Polym. Sci. 000: 000–000, 2013

KEYWORDS: electrochemistry; gels; properties and characterization

Received 15 April 2013; accepted 22 July 2013; Published online
DOI: 10.1002/app.39784

INTRODUCTION

In recently, supercapacitors with gel polymer electrolyte (GPE) has attracted much attentions because of their high reliability, flexibility, facile designing, separator-free and being free of the drawbacks of liquid electrolytes, such as leakage, volatilization, and corrosion, which can meet the increasing reliability demands of their practical applications.[1–4] In order to improve the electrochemical performance of the GPE, some modification methods have been utilized, such as the additions of the basic or acidic salt to enhance the conductivity because of the high dynamics of hydroxyl or proton (e.g., KOH and H_2SO_4),[1,5] and the incorporation of the redox mediator to bring the additional pseudocapacitance by the quick reversible redox reaction.[6–9]

Many investigations indicate that the properties of supercapacitors can be improved by adding the various electrochemically active compounds into the electrolytes, such as KI aqueous solution,[10] Cu^{2+} synergistic Fe^{2+} ions,[11] hexacyanoferrate (II) and (III),[12] hydroquinone,[13] iodide/vanadium conjugated redox couple,[14] phenylenediamine,[15,16] are proved to be effective active compounds for the enhancement of supercapacitors properties. Recently, Roldan et al. investigated MWCNT-based supercapacitors by containing methylene blue (MB) as redox active electrolyte, the results show that a cell capacitance was prominently enhanced by MB redox reaction. But, it was also found that MB cannot pass through the commonly used separator, Nafion membrane, which may hinder the ion transfer of electrolytes.[17] Considering GPEs-based supercapacitors are free of separator,[1] MB probably can be an appropriate mediator for GPEs.

Among the various classifications of host polymers, polyvinyl alcohol (PVA) is a good candidate for GPEs because of its excellent chemical stability, mechanical property, and nontoxicity.[1,5] In our previous work, we have demonstrated the performance of supercapacitors with I^-/I_2 redox couple and p-benzenediol in the PVA-based GPEs.[8,9] In this work, we make an attempt to incorporate redox mediator MB into polyvinyl alcohol/polyvinyl pyrrolidone (PVA/PVP) blend host to prepared a GPE (PVA-PVP-H_2SO_4-MB) for supercapacitors. This work is focused on the effect of MB on the performance of the supercapacitors and it was found that, with the addition of MB, the ionic conductivity of GPEs was improved, the electrical contact between the electrode and electrolyte was promoted, and the energy output of cell was enhanced.

EXPERIMENTAL

Materials

Activated carbon (AC), polytetrafluoroethylene (PTFE), and stainless-steel net were purchased commercially from Fuzhou Yihuan, Guangzhou Xingshengjie Science Technology, and

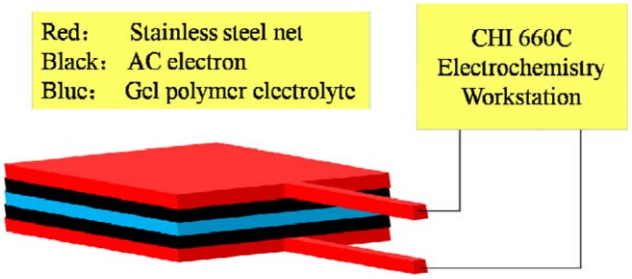

Figure 1. Schematic representation for the quasi-solid-state supercapacitor model. [Color figure can be viewed in the online issue, which is available at wileyonlinelibrary.com.]

Anping Ruiqi Wiremesh, respectively. Graphite, sulphuric acid (H_2SO_4), N-methyl-2-pyrrolidone (NMP), MB, polyvinyl pyrrolidone (PVP K-30, average molecular weight 58,000), and PVA (average molecular weight 88,000) were purchased from Sinopharm Chemical Reagent. All materials were commercially available and employed without further purification.

Preparation of GPEand AC Electrode

A PVA-PVP-H_2SO_4-MB GPE was prepared as described in previous literature.[8,18] A mixture of 1 g PVA and 0.4 g PVP, in which, PVP was introduced to enhance the plasticity of the polymer host, was dissolved in 20 ml deionized water with agitation at 50°C for 4 h, until a homogeneous and low-viscous solution was formed, and then an adequate amount of H_2SO_4 (0.01 mol) was added to the solution with a constant stirring rate. After 1 h, MB (0–0.5 g) was added into the above solution. Finally, the solution was evaporated at room temperature, and PVA-PVP-H_2SO_4-MB GPE was obtained. For the comparison, PVA-PVP-H_2SO_4 GPE was also prepared by the same method as described above without the addition of MB.

The AC electrode composed of AC, graphite and PTFE aqueous solution with weight ratio of 85:10:5 was prepared by following typical steps: AC, graphite and PTFE were dispersed in NMP at room temperature, the mixture was stirred continuously to form carbon paste, and then the carbon paste was pressed by Decal method to prepare a thin sheet.

The sheet with a fixed surface area of 0.5 cm^2 was pasted on current collector under pressure of 10 MPa. After being dried at 60°C for 24 h, an AC electrode was obtained. Meanwhile, each electrode processes the same mass of 2.5 mg.

Fabrication of Supercapacitor

A supercapacitor was fabricated by sandwiching the GPE between the two AC electrodes as shown in Figure 1. The two stainless-steel nets were used as current collectors. The GPE simultaneously served as separator and electrolyte. Furthermore, the SCs with PVA-PVP-H_2SO_4 GPE or PVA-PVP-H_2SO_4-MB GPE were hereinafter abbreviated as PPSC, MBPPSC, respectively.

Characterization

All the electrochemical tests were studied in a two-electrode system carrying out by an electrochemistry workstation (CHI 660C, Shanghai Chen Hua) under ambient conditions. The cyclic voltammetry (CV) measurements were performed in the potential range of 0–1 V at various scan rates from 2 to 50 $mV \cdot s^{-1}$. The galvanostatic charge–discharge (GCD) tests were measured with a different current density at cell voltages of 0–1 V. Moreover, the electrode specific capacitance (C_g, $F \cdot g^{-1}$), as well as the equivalent series resistance (ESR, Ω), energy density

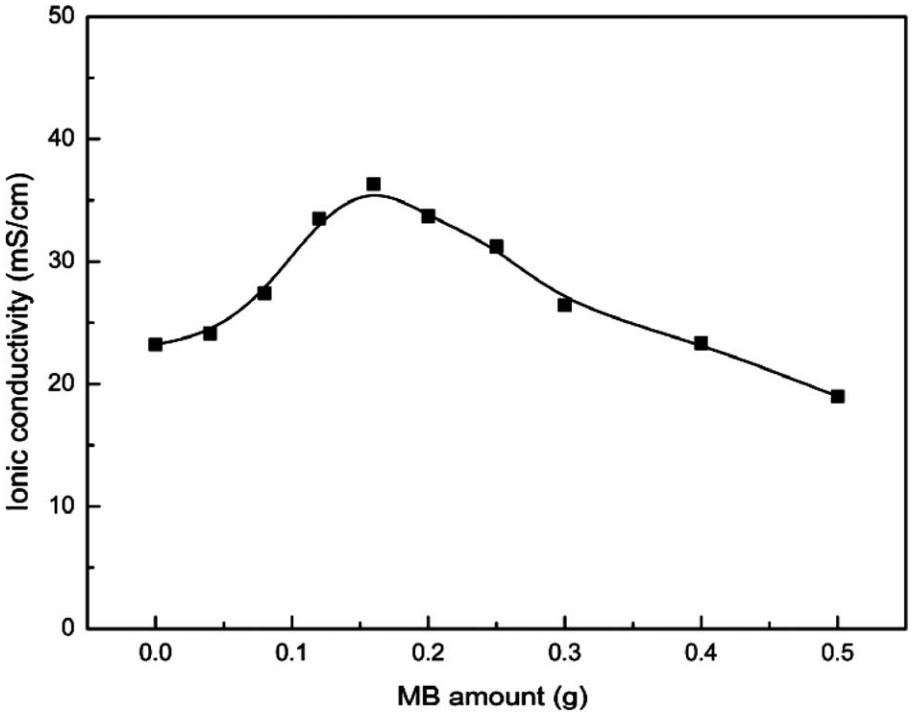

Figure 2. Ionic conductivity of PVA-PVP-H_2SO_4-MB GPE with different amount of MB.

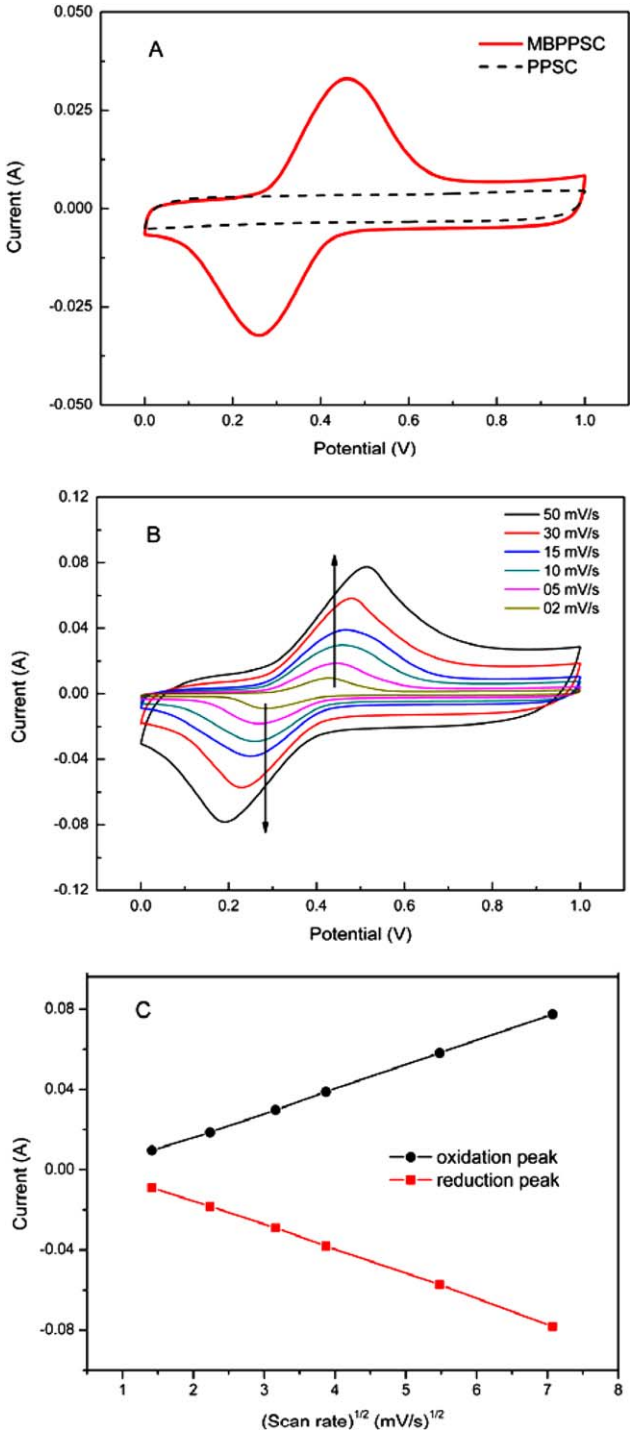

Figure 3. (A) The capacitive performance of MBPPSC and PPSC at a scan rate of 10 mV·s^{-1} in 0–1 V. (B) CV curves of MBPPSC at different scan rates from 2 to 50 mV·s^{-1} in 0–1 V. (C) The dependence of the cathodic and anodic peak currents on the scan rate for MBPPSC. [Color figure can be viewed in the online issue, which is available at wileyonlinelibrary.com.]

(E, Wh·kg^{-1}) and power density (P, kW·kg^{-1}) of cell were both evaluated from charge-discharge curves.[15] The electrochemical impedance spectroscopy (EIS) techniques were evaluated over the frequency ranging from 100 kHz to 10 mHz with a bias voltage of 0 V. The ionic conductivity of GPEs was measured by a conductivity meter (DDSJ-308A, Shanghai REX Instrument Factory).

RESULTS AND DISCUSSION

The Ionic Conductivity of GPE

The ionic conductivity of GPE is crucial to the performance of supercapacitors. The dependence of MB amount on the ionic conductivity of GPE is shown in Figure 2. The ionic conductivity of GPE increases with the increase of MB amount and reaches to the highest value of 36.3 mS·cm^{-1} at 0.16 g of MB, and then decreases gradually with the increase of MB amount, which means that the ionic conductivity of GPE can be improved with the appropriate doping amount of MB. It is probably because of the quick reversible redox processes triggered by MB, making the ionized MB provide more valid ions transferring through the free volume in the polymer host,[5] and the corresponding processes are presented in the following equation:

$$AX + A \leftrightarrow AX + A \quad (1)$$

where A is the reduced state of the MB species, AX is the oxidized state of the MB species, X is a molecule, ion, radical, or energy quantum.[19] The net effect is that A and AX exchange their positions and translate a step to the left and right, respectively. This effect makes the ionic conduction more efficient. However, the superfluous doping amount of MB will lead to the aggregation of free ions in the polymer matrix, which impeded the ions transport and induced the decrease of ionic conductivity.[20]

CV Measurements

Figure 3(A) shows the CV behavior of MBPPSC and PPSC at a scan rate of 10 mV·s^{-1}. The curve of PPSC reveals a near rectangle shape, which is approximated to the ideal situation of electrical double layer capacitor,[13] implying that charge and discharge occurred reversibly at electrodelelectrolyte interface, and the corresponding electrical double layer forming processes are presented in the following equation:

$$C + H^+ + e^- \leftrightarrow C^-//H^+ \quad (2)$$

When the MB was introduced to the PVA-PVP-H_2SO_4 system, a pair of remarkable and symmetric redox peaks appears because of Faradaic reactions occurring on the positive and negative electrodes. Obviously, MBPPSC has higher capacitance values than PPSC, being attributed to the coexistence of the double-layer capacitance of porous carbon materials and pseudocapacitance contribution from the Faradaic processes of redox mediator.[21] As described elsewhere,[17,22] the probably mechanism of the electronic processes of redox reactions are presented in Figure 4. In simplest terms, these are reversible hydrogenation–dehydrogenation reactions, between the oxidation and reduction of MB. Typically, as a pH dependent redox mediator, the formal potential of MB, E^0, is between 0.532 and 0.011 V [vs. Standard Hydrogen Electrode (SHE)] in the solution with pH between 0 and 7.[23] Herein, the oxidation and reduction peak potentials in

Applied Polymer SCIENCE

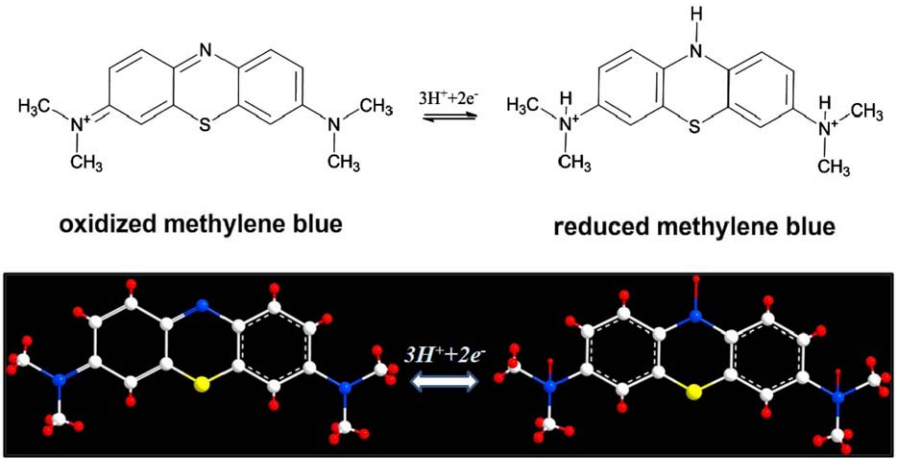

Figure 4. Representation of the redox processes in the electrodelelectrolyte system. [Color figure can be viewed in the online issue, which is available at wileyonlinelibrary.com.]

the CV graphs are denoted as E_O (0.457 V) and E_R (0.263 V), respectively. The smaller $E_O - E_R$ (ΔE) value is a measure of better reversibility in the redox reaction.[24] From Figure 3(A), it is found that MBPPSC exhibits a normal ΔE (194 mV) at the scan rate of 10 mV·s^{-1}, compared to the iodide/vanadium conjugated redox couple,[14] implying high-reversibility of redox reaction at the electrodelelectrolyte interface.

Figure 3(B) presents the CV curves for MBPPSC at different scan rates from 2 to 50 mV·s^{-1}. The series of CV curves show pronounced current response over the potential window with the reductive peaks shifting positively and the oxidative peaks shifting negatively with the increase of the scan rates, which is mainly related to the internal resistance of the electrode. Moreover, with the increase of the scan rates, the redox peaks tended towards gentle, suggested that the Faradaic processes are restricted by rather slow diffusion and require time to trigger, particularly at a high scan rate.[13] On the whole, the CV profiles removed the bumps obscurely, which still retained the initial shape without significant distortion with the increasing potential scan rates, demonstrating excellent high-rate performance.

In order to further analyze CV characteristic of MBPPSC, the responses of the cathodic and anodic peak currents to sweep rates (2–50 mV·s^{-1}) were measured. It can be seen from Figure 3(C) that either the oxidation peak current (i_{op}) or reduction peak current (i_{rp}) vs. scan rate$^{1/2}$ plot, give a reasonable linear relationship, respectively. These behaviors can be suggested that the oxidation and reduction of MB are diffusion-controlled processes.[25]

GCD Tests

The resistance and capacitance of PPSC and MBPPSC were evaluated by GCD tests and shown in Figure 5. As can be seen from the GCD curves, the PPSC displays a linear charge–discharge behavior. On the other hand, after adding MB to PPSC, the MBPPSC displays a nonlinear charge–discharge behavior, which is because of the pseudopotential by MB. The electrochemical behavior in the charge process from 0 to 0.4 V and the discharge process from 0.4 to 0 V mainly come from the MB pseudocapacitance contribution, and the electrochemical behavior in the charge process from 0.4 to 1.0 V and the discharge process from 1.0 to 0.4 V mainly come from the GPE double layer capacitance contribution, which is in good agreement with the CV measurement results shown in Figure 3. Because of these additional redox reactions, the charge–discharge time of MBPPSC is prolonged. Moreover, MBPPSC exhibits a smaller iR_{drop} than PPSC, and the ESR are calculated as 2.37 and 6.79 Ω·cm^2, respectively. The ESR is the sum of the intrinsic resistance of all materials and the contact resistance between them. The reduction of that probably because of: (a) the improvement of the ionic conductivity of GPEs; and (b) the enhanced conjunction between GPE and electrodes via electron transfer between the mediators.

The electrode specific capacitances (C_g) for MBPPSC and PPSC are calculated to be 328 and 124 F·g^{-1} at the current density of 1 A·g^{-1}, respectively. Obviously, the C_g of MBPPSC is larger than that of PPSC, indicating that the redox mediator MB can greatly improve the capacitive property of the supercapacitor. The capacitance values and retention ratio of the AC electrode

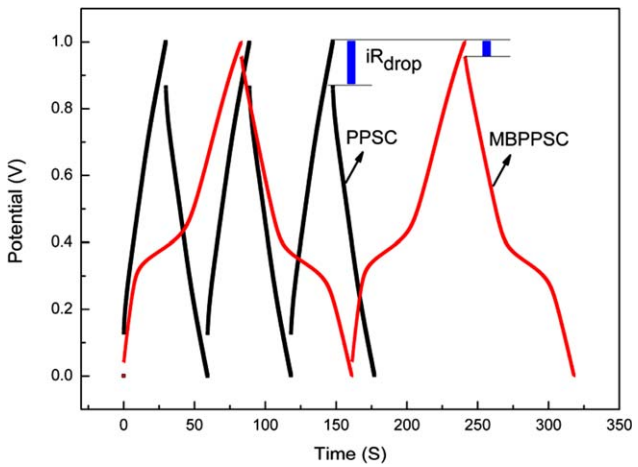

Figure 5. GCD curves of MBPPSC and PPSC, charge-discharge current density: 1 A·g^{-1}. [Color figure can be viewed in the online issue, which is available at wileyonlinelibrary.com.]

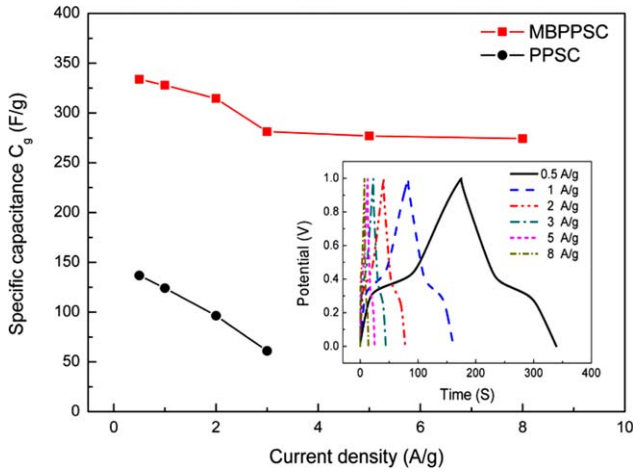

Figure 6. C_g of MBPPSC and PPSC at different charge–discharge current density. The inset shows the corresponding GCD curves of MBPPSC. [Color figure can be viewed in the online issue, which is available at wileyonlinelibrary.com.]

are shown in Figure 6, and the inset shows the corresponding GCD curves of MBPPSC. The C_g of MBPPSC at current densities of 0.5, 1, 2, 3, 5, and 8 $A \cdot g^{-1}$ are calculated to be 334, 328, 314, 281, 277, and 274 $F \cdot g^{-1}$, respectively. Similarly, the C_g of PPSC at current densities of 0.5, 1, 2, and 3 $A \cdot g^{-1}$ are 137, 124, 96, and 61 $F \cdot g^{-1}$, respectively. It can be observed that both the C_g of PPSC and MBPPSC decreased with the increase of current density from 0.5 to 3 $A \cdot g^{-1}$, respectively, and the C_g values of MBPPSC are larger than those of PPSC in whole current density range. Interesting, the C_g values of MBPPSC decrease with the increase of current density when current density is lower than 4 $A \cdot g^{-1}$, but it almost kept stable when increase current density from 4 to 8 $A \cdot g^{-1}$. The former is because of the GPE double layer capacitance, similar to the PPSC system and the latter is because of the MB pseudocapacitance.

The Ragone plots showing the dependence between power output and energy density are displayed in Figure 7. At the same current density of 0.5 $A \cdot g^{-1}$, the calculated energy densities of MBPPSC and PPSC are ca. 11.2 and 4.0 $Wh \cdot kg^{-1}$, respectively, and the corresponding power densities are 246 and 230 $W \cdot kg^{-1}$, respectively. At the same current density of 3 $A \cdot g^{-1}$, the calculated energy density and power density of MBPPSC are 8.1 and 1369 $W \cdot kg^{-1}$, respectively, and those of PPSC are 0.8 and 845 $W \cdot kg^{-1}$, respectively. It is noted that MBPPSC has a higher energy and power density than PPSC, and the latter represents a normal level.[26]

EIS Techniques

In order to investigate the electrochemical behavior at the electrode|electrolyte interface in detail, EIS measurements were employed. Figure 8 shows the Nyquist plots for MBPPSC and PPSC. They both have ideal electrochemical capacitance behavior, i.e., a small depressed semicircle at higher frequency, imaginary part of impedance at low frequency region being perpendicular to the real part.[27]

From the enlarged view of the higher frequency semicircles, it can be seen that MBPPSC not only has lower inner resistance (R_i, 0.42 $\Omega \cdot cm^2$), calculated from the point of intersecting with the x-axis in the range of high frequency, but also has smaller charge transfer resistance (R_{ct}, 1.84 $\Omega \cdot cm^2$), counted from the

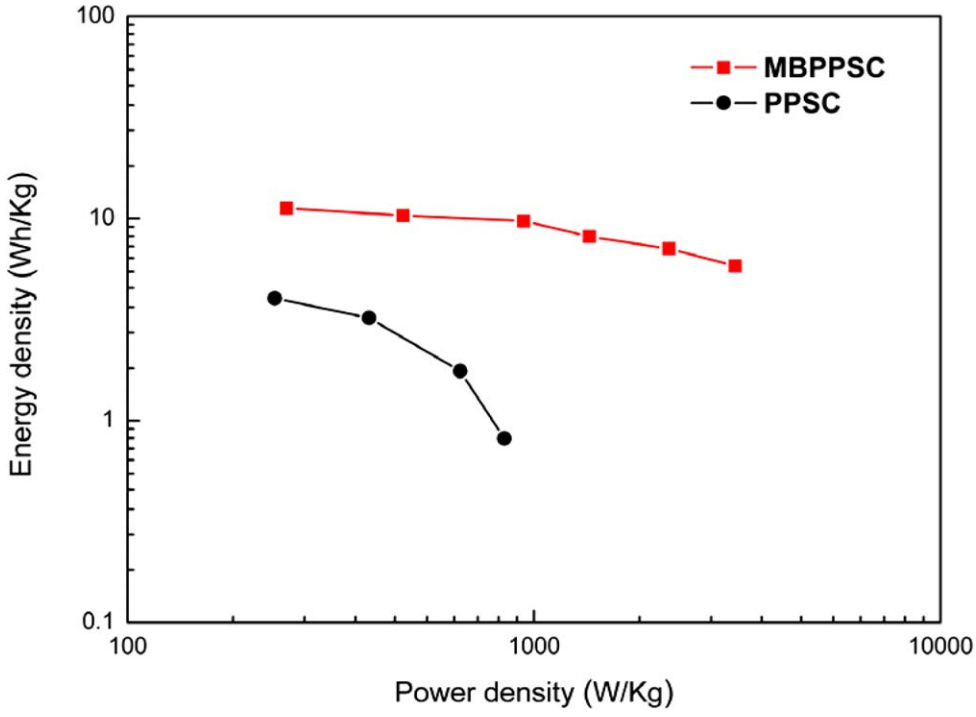

Figure 7. Ragone plots related to energy and power densities of MBPPSC and PPSC. [Color figure can be viewed in the online issue, which is available at wileyonlinelibrary.com.]

Applied Polymer SCIENCE

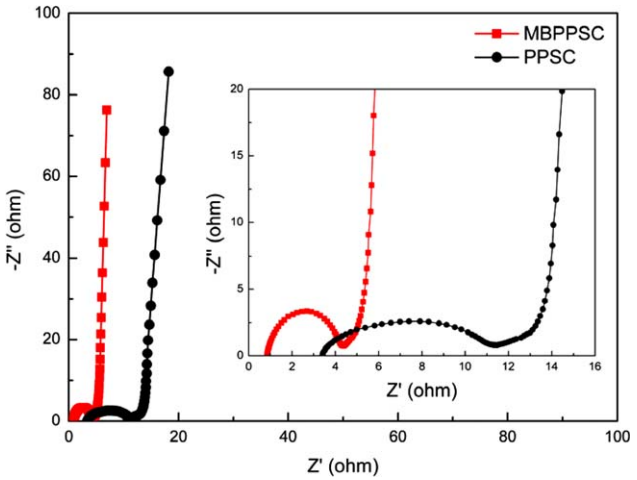

Figure 8. EIS of MBPPSC and PPSC, the close-up view of the left plot in high-frequency region. [Color figure can be viewed in the online issue, which is available at wileyonlinelibrary.com.]

span of the single semicircle along the *x*-axis from high to low frequency. Hence, the MB mediator can enhance the interaction of electrodelelectrolyte interface, which results in good electrochemical performance for PVA-PVP-H_2SO_4-MB GPE system.

Moreover, from the discussions both of CV and GCD measurements, they imply that MBPPSC has higher specific capacitance as well as better electrochemical properties than PPSC. The same results also can be deduced from the frequency-dependant capacitance of supercapacitors. In the plots of capacitance vs. frequency, C' (F) represents the real part of the capacitance, C'' (F) is the imaginary part of the capacitance, f_k (Hz) is the knee-frequency, τ(s) is the relaxation time when system obtained the frequency f_k.[28]

From Figure 9A, the value of C' for MBPPSC is obviously higher than that of PPSC, they started with 361 and 149 $F{\cdot}g^{-1}$ at 10 mHz, respectively. Meanwhile, from Figure 9(B), the dotted lines reveal that the peak maximum of f_k for MBPPSC shifts to higher. Such raise of the f_k might be attributed to the additional reversibility, which is provided by the reversible redox reactions of MB. On the other hand, the dielectric relaxation time (τ) is determined by the f_k, of which the smaller value represents the less time of supercapacitor reach the half of the low frequency capacitance implying the better power properties of the system. The τ of MBPPSC was calculated as 8.5 s, which is lower than that of PPSC (10.2 s). Thus, it implies that the redox-active GPE is more suitable for supercapacitor.

Self-Discharge Testing

Self-discharge is an important parameter for the electrochemical energy-storage device. The open-circuit voltage of MBPPSC and PPSC were monitored and the results were shown in Figure 10. At the beginning of about 5 h, both of supercapacitors undergo a rapid self-discharge course, and then display a much lower discharge rate. After 24 h, MBPPSC and PPSC enter a discharge plateau of ca. 0.31 and 0.27 V, respectively. This implies that capacitance accumulated in such a hybrid system can be stored for longer and the introduction of MB additive is an acceptable way for improving the performance of supercapacitor.

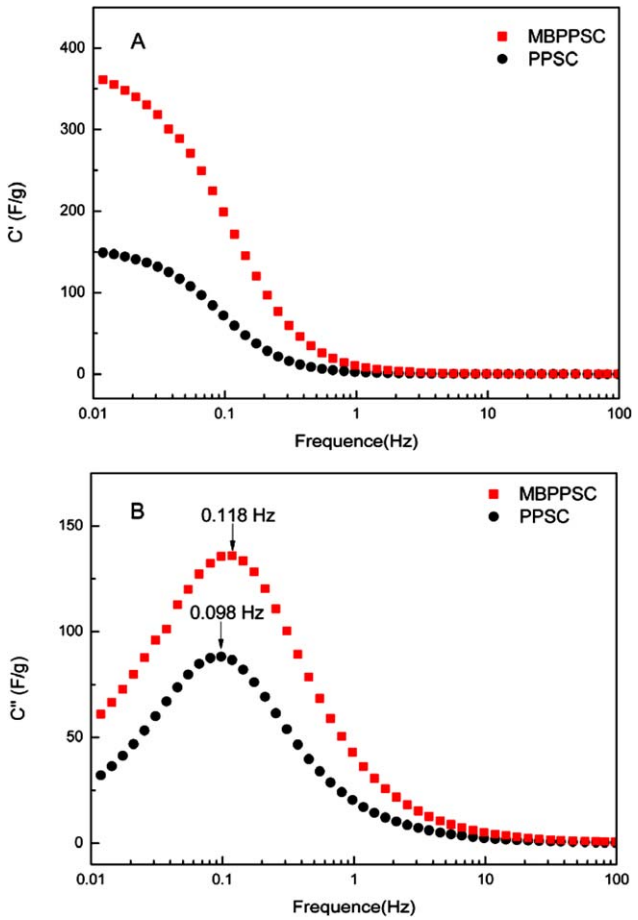

Figure 9. (A) Evolution of the real part of the capacitance vs. the frequency of MBPPSC and PPSC. (B) Variation of the imaginary part of the capacitance vs. the frequency of MBPPSC and PPSC. [Color figure can be viewed in the online issue, which is available at wileyonlinelibrary.com.]

Cycle Life Test

Cyclic durability is one of the most significant electrochemical performances of supercapacitor. Herein, GCD tests were carried

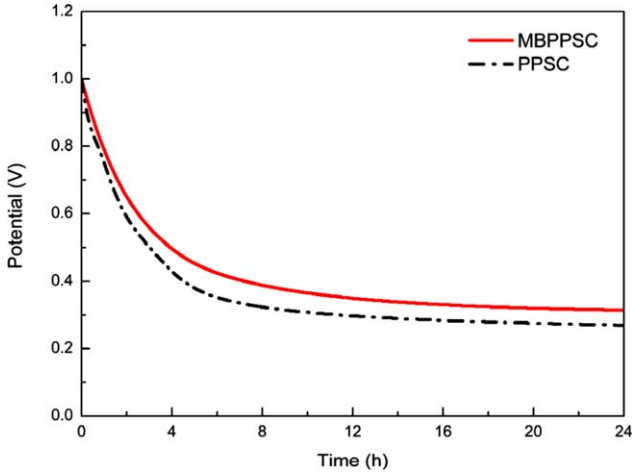

Figure 10. Self-discharge curves of MBPPSC and PPSC. [Color figure can be viewed in the online issue, which is available at wileyonlinelibrary.com.]

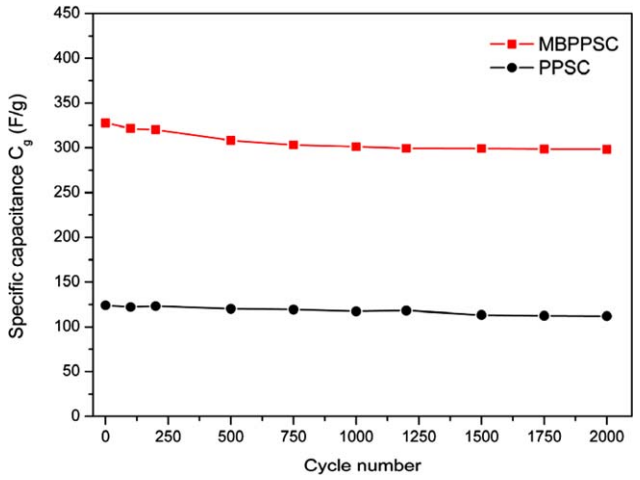

Figure 11. The C_g of MBPPSC and PPSC during long-term cycling. [Color figure can be viewed in the online issue, which is available at wileyonlinelibrary.com.]

out at a constant charge–discharge current density of 1 $A \cdot g^{-1}$ and the plots of specific capacitances of PPSC and MBPPSC as a function of charge–discharge cycles are shown in Figure 11. After 2000 charge–discharge cycles, the C_g of PPSC decreases from 124 to 112 $F \cdot g^{-1}$, and the C_g of MBPPSC decreases from 328 to 298 $F \cdot g^{-1}$, still retains 90% and 91 % of the initial capacitance for PPSC and MBPPSC, respectively. It can be concluded that a redox-active MB doping not only can increase the C_g of supercapacitor, but also scarcely impede the stability of supercapacitors, indicating that the PVA-PVP-H_2SO_4-MB GPE can be considered as a promising GPE in supercapacitor.

CONCLUSIONS

In summary, we have demonstrated the feasibility of a carbon-based supercapacitor utilizing a redox-active GPE (PVA-PVP-H_2SO_4-MB). With the contribution of the redox reaction of MB and its quick electron relay at the electrodelelectrolyte interface, the supercapacitor shows excellent electrochemical performance, such as, high electrode specific capacitance of 328 $F \cdot g^{-1}$, high energy density of 10.3 $Wh \cdot kg^{-1}$, and excellent cycle life that maintains 91% of the initial capacitance values of after 2000 cycles. Therefore, it is an effective way to enhance the electrochemical performance of supercapacitor by using redox-active GPEs.

ACKNOWLEDGMENTS

The authors acknowledge the financial joint support by the National Natural Science Foundation of China (Nos. U1205112, 50842027) and the specialized research fund for the doctoral program of Higher University, Ministry of Education, China (No. 20123501110001).

REFERENCES

1. Choudhury, N.; Sampathb, S.; Shukla, A. *Energ. Environ. Sci.* **2009**, *2*, 55.
2. Reiter, J.; Vondrak, J.; Michalec J.; Micka, Z. *Electrochim. Acta* **2006**, *52*, 1398.
3. Ryu, K.; Wu, X.; Lee, Y.; Chang, S. *J. Appl. Polym. Sci.* **2003**, *89*, 1300.
4. Kumar, M.; Bhat, D. *J. Appl. Polym. Sci.* **2009**, *114*, 2445.
5. Choudhury, N.; Shukla, A.; Sampath, S.; Pitchumani, S. *J. Electrochem. Soc.* **2006**, *153*, A614.
6. Yin, Y.; Zhou, J.; Mansour, A.; Zhou, X. *J. Power Sources* **2011**, *196*, 5997.
7. Zhou, J.; Cai, J.; Cai, S.; Zhou, X.; Mansour, A. *J. Power Sources* **2011**, *196*, 10479.
8. Yu, H.; Wu, J.; Fan, L.; Xu, K.; Zhong, X.; Lin, Y.; Lin, J. *Electrochim. Acta* **2011**, *56*, 6881.
9. Yu, H.; Wu, J.; Fan, L.; Lin, Y.; Xu, K.; Tang, Z.; Cheng, C.; Tang, S.; Lin, J.; Huang, M.; Lan, Z. *J. Power Sources* **2012**, *198*, 402.
10. Lota, G.; Frackowiak, E. *Electrochem. Commun.* **2009**, *11*, 87.
11. Li, Q.; Li, K.; Sun, C.; Li, Y. *J. Electroanal. Chem.* **2007**, *11*, 43.
12. Su, L.; Zhang, X.; Mi, C.; Gao, B.; Liu, Y. *Phys. Chem. Chem. Phys.* **2009**, *11*, 2195.
13. Roldan, S.; Blanco, C.; Granda, M.; Menendez, R.; Santamaria, R. *Angew Chem. Int. Ed.* **2011**, *50*, 1699.
14. Frackowiak, E.; Fic, K.; Meller, M.; Lota, G. *ChemSusChem* **2012**, *5*, 1181.
15. Wu, J.; Yu, H.; Fan, L.; Luo, G.; Lin, J.; Huang, M. *J. Mater. Chem.* **2012**, *22*, 19025.
16. Yu, H.; Wu, J.; Lin, J.; Fan, L.; Huang, M.; Lin, Y.; Li, Y.; Yu, F.; Qiu, Z. *ChemPhysChem* **2013**, *14*, 394.
17. Roldan, S.; Granda, M.; Menendez, R.; Santamaria, R.; Blanco, C. *Electrochim. Acta* **2012**, *83*, 241.
18. Wu, J.; Li, P.; Hao, S.; Yang, H.; Zhang, L. *Electrochim. Acta* **2007**, *52*, 5334.
19. Ruff, I.; Friedrich, V. *J. Phys. Chem.* **1971**, *75*, 3297.
20. Ramesh, S.; Liew, C.; Ramesh, K. *J. Appl. Polym. Sci.* **2013**, *127*, 2380.
21. Conway, B.; Birss, V.; Wojtowic, J. *J. Power Sources* **1997**, *66*, 1.
22. Arvand, M.; Sohrabnezhad, S.; Mousavi, M.; Shamsipur, M.; Zanjanchi, M. *Anal. Chim. Acta* **2003**, *491*, 193.
23. Tratnyek, P.; Reilkoff, T.; Lemon, A.; Scherer, M.; Balko, B.; Feik, L.; Henegar, B. *Chem. Educator* **2001**, *6*, 172.
24. Meher, S.; Justin, P.; Rao, G. *Nanoscale* **2011**, *3*, 683.
25. Wang, Y.; Hong, Z.; Wei, M.; Xia, Y. *Adv. Funct. Mater.* **2012**, *22*, 5185.
26. Wada, H.; Yoshikawa, K.; Nohara, S.; Furukawa, N.; Inoue, H.; Sugoh, N.; Iwasaki, H.; Iwakura, C. *J. Power Sources* **2006**, *159*, 1464.
27. Taberna, P.; Simon, P.; Fauvarque, J. *J. Electrochem. Soc.* **2003**, *150*, A292.
28. Zeller, M.; Lorrmann, V.; Reichenauer, G.; Wiener, M.; Pflaum, J. *Adv. Energy Mater.* **2012**, *2*, 598.